Crystallization Behavior of Polyethylene Oxide/ *Para*-Nitroaniline Microdispersed Composites

C. SAUJANYA, S. RADHAKRISHNAN

Polymer Science and Engineering, National Chemical Laboratory, Pune 411 008, India

Received 14 May 1996; accepted 25 November 1996

ABSTRACT: The crystallization behavior of polyethylene oxide (PEO) containing microdispersed nonlinear optical chromophores such as *para*-nitroaniline (PNA) has been investigated with respect to comopsition and different methods of film preparation techniques viz. solvent casting, melt casting, and powder molding. Large variations in the intensities of major reflections, 012 and 101, from PNA crystallites were observed depending on the composition as well as the method of preparation. The morphology of the samples examined under cross-polarizing conditions revealed highly birefringent crystallites dispersed in the spherulitic morphology of the PEO matrix in contrast to weakly birefrindgent crystals of the additive by itself. At high concentrations exceeding 45 wt % the PNA crystals act as substrates for the growth of polymer crystals. These results have been explained on the basis of intermolecular interaction as well as good lattice match between the crystalizing components, leading to preferential growth of the crystals along a certain direction. © 1997 John Wiley & Sons, Inc. J Appl Polym Sci **65:** 1127–1137, 1997

Key words: non-linear optical materials; microdispersed composites; PEO/PNA guest–host system

INTRODUCTION

Materials exhibiting nonlinear optical (NLO) properties have been drawing considerable attention in recent years because of their potential application in optoelectronic devices.[1–3] Many polymers as well as organic compounds have been investigated in the past in this respect.[3–5] Among the various materials, those based on nitroaniline derivatives have been studied extensively both as single crystals and as polymer-dispersed guest/host systems.[6–8] Interestingly *para*-nitroaniline (PNA), although it does not exhibit second-order effect by itself, has been reported to be nonlinearly optically active when dispersed in polymers such as aliphatic polyesters, ultraviolet-cured polyacrylates, and polyethers.[9–12] The long-term stability of NLO properties in such polymer-dispersed systems has been found to be unsatisfastory and attributed to large-scale disordering of originally oriented molecules. Further, most of the polymers used in the past were amorphous, having large free volume and a high degree of freedom for molecular motion. It was felt that by using semicrystalline polymers, it may be possible to restrict this motion and improve the stability of the properities. It may also be possible to induce oriented growth of crystals by either appropriate processing or by the process of polymer-induced crystallization.[13,14] However, for the latter process to take place, the polymer can interact with the guest molecules through charge transfer (donor-acceptor type or hydrogen bonding would be necessary). Hence, polyethylene oxide (PEO), which is known to form complexes with a large number of materials including urea (via NH_2 group), was

Correspondence to: S. Radhakrishnan.

chosen for these studies. We found very interesting crystallization behavior and morphological features in such systems, and these are described in this article.

EXPERIMENTAL

PEO (polyox WSR; BDH, England; $M_w = 3 \times 10^5$) was dissolved in methanol along with the required quantity of PNA (BDH) so as to form clear solutions indicating no turbidity or immiscibility at any range of compositions. These were cast on microscopic glass slides or flat Petri dishes so as to facilitate microscopic observations. The films were kept in a dry box at 35°C for a period of 24 h so as to remove the solvent completely. The optical quality of the films ranges from transparent clear to dense opaque, depending on the composition. These are designated as solution-crystallized films (SC). Some of these films were placed between glass slides and subjected to melt crystallization by first melting at 150°C followed by isothermal crystallization in the hot stage of the microscope at 40°C. These are designated as melt-crystallized samples (MC). A few compositions were also made by dry powder mixing the components in an agate pestle mortar followed by high-pressure, 3,000 kg/cm^2 compression molding and melt crystallization between Teflon sheets. These are termed as powder-crystallized samples (PC) in the text. The crystalline structure, phase, and morphology were investigated by X-ray diffraction and optical polarizing microscopy in the same manner as reported elsewhere.[15,16]

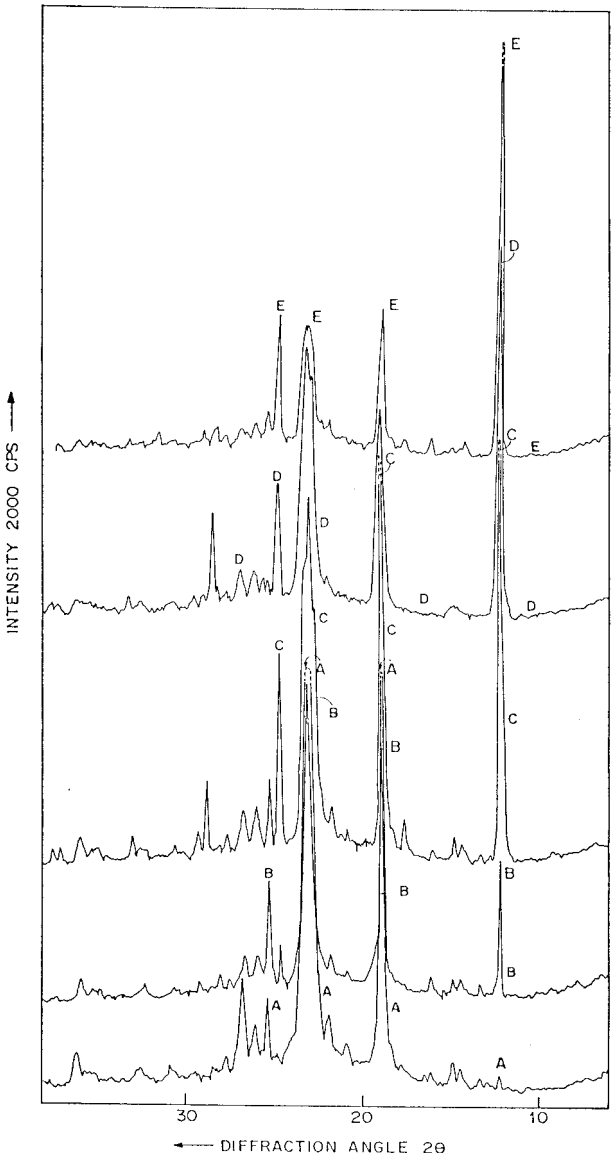

Figure 1 WAXD scans for PEO-PNA (SC) samples with different concentrations of PNA. Curves A–E correspond to PNA concentrations of 10, 15, 35, 45, and 50% by weight, respectively.

RESULTS AND DISCUSSION

The wide-angle X-ray diffraction (WAXD) of these samples reveals some interesting features. Figure 1 shows the WAXD of (SC) samples with different concentrations of PNA; curves A to E correspond to PNA concentrations of 10, 15, 35, 45, and 50 by weight, respectively. Comparing these with the WAXD of pure PNA and PEO [Fig. 2(a) and (b), respectively], it is seen that a very large increase or decrease of intensities for some of the peaks is observed in PEO-PNA. The d values and the relative intensities derived from these data are shown in Tables I and II. These various values indicate that the crystalline phases of PNA and PEO in the (SC) samples are same as that of the original components, but the relative intensities of the peaks, especially those corresponding to 101 and 012 reflections of PNA, are distinctly different in the (SC) samples. It may be noted that PNA itself exhibits a very intense peak in its WAXD, designated here as peak 1 [see Fig. 2(a)] corre-

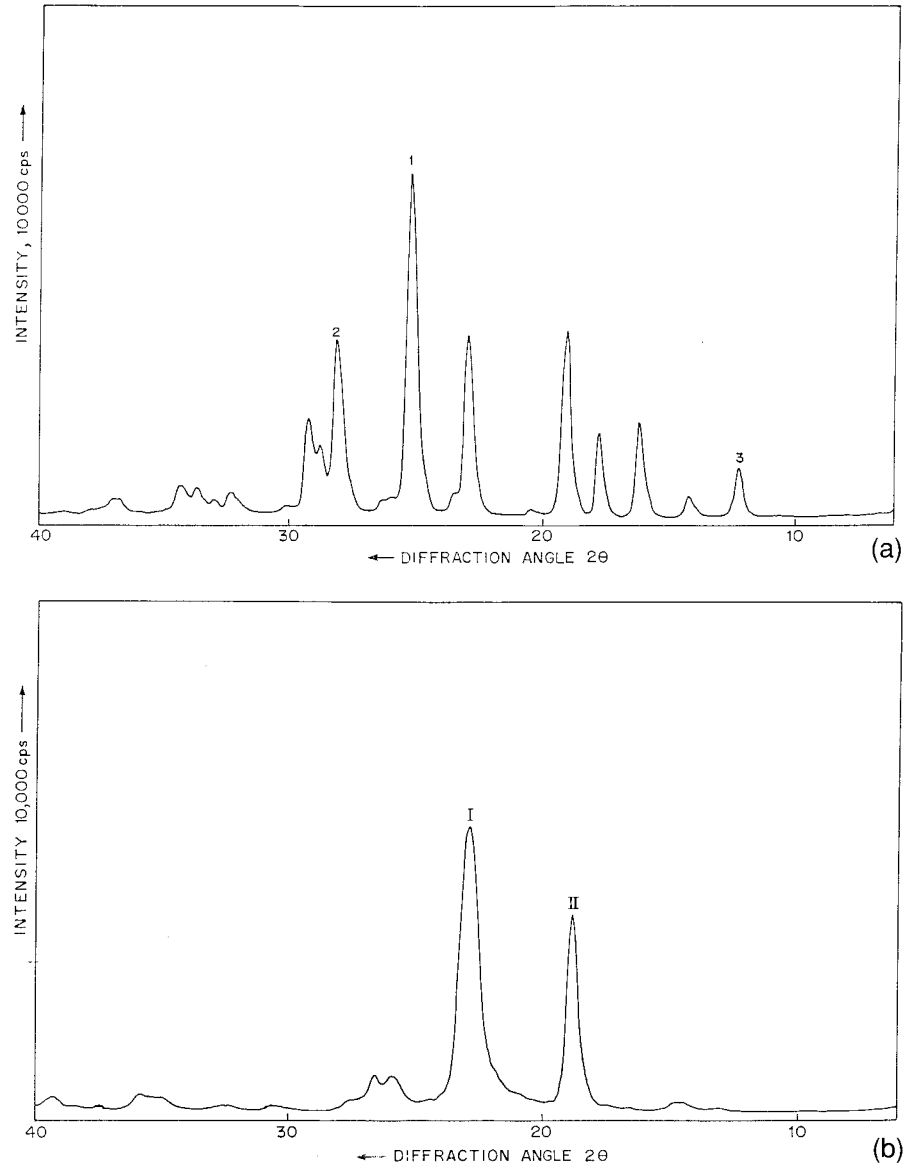

Figure 2 (a) WAXD scan for pure PNA; (b) WAXD scan for pure PEO.

sponding to the 012 reflection. Additionally, we have considered two peaks, peak 2 and peak 3, which correspond to 020 and 101 reflections from PNA and which do not overlap on the PEO peaks. Similarly, PEO by itself exhibits two intense peaks in its X-ray diffraction which have been designated as peak I and peak II [see Fig. 2(b)]. In pure PEO, peak I has a much higher intensity than peak II. The WAXD of PEO-PNA samples with a low concentration of PNA conformed to this. On the other hand, when PNA concentration is increased beyond 20%, there is a large change in the relative intensities of these peaks and peak II has a much higher intensity than peak I. The intensities of major reflections from PNA crystallites in the PEO-PNA composite films are also distinctly different from those in pure PNA. In the latter case, peak 1 has the strongest intensity and peak 3 has a minor one. On the other hand, in PEO-PNA (SC) samples, peak 1 of PNA has quite a low intensity while peak 3 has the highest. This suggests that a

Table I X-Ray Diffraction in PEO-PNA Grown by Solution Cast Technique

PEO-PNA Compositions										Remarks	
10%		15%		35%		45%		50%		PNA	Peo
d (obs)	*I/Io*	*d* (obs)	*I/Io*	*d* (obs)	*I/Io*	*d* (obs)	*I/Io*	*d* (obs)	*I/Io*	*hkl*	*hkl*
7.20	3	7.20	43	7.20	100	7.20	100	7.20	100	101	
6.61	2	6.61	4								
								6.19	3		021
6.11	4	6.11	6	6.07	2					010	
5.91	5	5.91	5	5.91	3	5.95	4	5.91	2		110
5.47	4	5.47	7	5.47	1			5.51	4	110	
4.98	5			4.98	5			5.04	3	011	
4.67	88	4.67	80	4.67	58	4.65	54	4.67	31	111	120/111
4.23	9	4.23	9	4.23	4					002	
4.04	14			4.06	7	4.02	11	4.06	7	102	
				3.85	45	3.85	64	3.85	25	211	
3.81	100	3.81	100	3.80	35	3.81	73	3.82	24		112
3.58	7	3.59	16	3.59	26	3.59	37	3.60	29	202	
3.51	17	3.51	36	3.51	10	3.50	11	3.52	9	012	
3.41	13	3.41	14	3.41	7	3.41	13	3.43	7	310	033
3.32	21	3.32	14	3.31	7	3.31	14	3.33	5	112	131
3.22	6	3.22	7	3.21	4	3.22	7	3.22	4	311	200
				3.08	10	3.13	28	3.07	4	400/212	
		3.03	6	3.04	4	3.03	7			020	
2.90	4			2.90	2	2.90	5			401/120	
								2.84	5	021	
2.75	4	2.76	5			2.74	5			121	211
				2.71	3	2.70	6			220	

As per the monoclinic structure of PNA: $a = 12.33$ Å, $b = 6.07$ Å, $c = 8.59$ Å, and $\beta = 91.45°$. As per the monoclinic structure of PEO: $a = 8.02$ Å, $b = 13.4$ Å, $c = 19.2$ Å, and $\beta = 126°$. obs, observed.

distinctly different type of growth pattern and/or orientation of crystallites with respect to film surface takes place in these samples.

The variation of intensities of the different WAXD peaks in PEO-PNA (SC) films with respect to composition is shown in Figure 3. It is seen that some of the peaks show a maximum at a particular concentration of about 35% PNA. If PEO-PNA had contained two phases with no interaction between them, that is, just a mixture of the two components existing independently, then there would not have been any change in the relative intensities of WAXD peaks with composition. Further, a decrease or increase of the concentration of one component would have caused a corresponding decrease or increase of intensity of WAXD peaks from that component. For example, one would have then expected the PEO peaks I and II to decrease in intensity monotonically with the increase of PNA concentration. Similarly the peaks 1, 2, and 3 of PNA would have increased in intensity without any change in the ratio of their relative intensities. However, the observations presented here show a distinctly different behavior. The intensity of peak I of PEO shows a continuous decrease in intensity, but the peak II does not. Even the major intense peak of PNA decreases drastically while a minor reflection peak 3 exhibits a maximum intensity in PEO-PNA samples. These peculiar findings can be understood in terms of the preferential growth and nucleation of crystallites along certain directions or their orientation, which are discussed later in the article.

Table II X-Ray Diffraction of Pure PNA and PEO

PNA 100%			PEO 100%		
d (cal)	*I/Io*	*hkl*	*d* (cal)	*I/Io*	*hkl*
7.12	15	101			
			6.18	5	021
			5.83	5	110
5.44	28	110			
4.96	25	011			
4.61	54	111	4.60	70	120/111
4.32	3	210			
3.88	54	211			
			3.82	100	112
3.74	8	301			
3.51	100	012			
3.40	6	310	3.40	14	033
3.38	6	112	3.34	14	131
3.18	52	311	3.24	5	200
3.07	21	212			
3.04	29	020			
2.95	4	120			
2.79	8	121	2.79	3	211
2.72	6	220			
2.63	9	411			
2.61	10	203			
2.44	6	320			

As per the monoclinic structure of PNA: a = 12.33 Å, b = 6.07 Å, c = 8.59 Å, and β = 91.45°. As per the monoclinic structure of PEO: a = 8.02 Å, b = 13.4 Å, c = 8.59 Å, and β = 126°. The peaks designated are as follows. PNA: peak 1, 012; peak 2, 212; and peak 3, 101 reflections. PEO: peak I, 112; and peak II, 111/120 reflections.

The PEO-PNA (MC) samples showed a different trend in the variation of the WAXD reflections than that noted in (SC) samples. Figure 4 depicts the WAXD scans for these samples, and Figure 5 shows the variation of intensities of corresponding peaks with respect to PNA concentration. In this case, it is seen that the intensities of PEO peak I decrease monotonically while PEO peak II shows a maximum in intensity (at 25%) with the increase of concentration of PNA. The PNA peaks, on the other hand, show little variation up to a concentration of 40% of PNA, above which there is a sudden increase in their intensities. Peak 3 of PNA in these (MC) samples does not show any prominence (compare Figs. 1 and 4). The PC exhibit a mixed trend. In this case (Fig. 6), the variation of intensities of peaks I and II of PEO are similar to those observed above but the PNA peak 3, which was weak in (MC) samples, appears quite prominent at all compositions studied (10–50% of PNA).

The morphology of these films varied considerably from those of individual components. PEO has a large spherulitic morphology [Fig. 7(a)], while PNA consists of small globular-type crystals [Fig. 7(b)]. Further, PNA shows only weak birefringence, that is, these crystals are not completely visible under cross-polarized conditions. On the other hand, the PEO-PNA composite films exhibit bright, shiny crystals which are placed in a spherulitic-like morphology. Figure 7(c) and (d) show the morphology of PEO-PNA (SC) films containing 10–30% PNA. It can be seen that the morphologies are PEO-like but that the internal structure of the spherulite is quite different. This is similar to the transcrystallinity observed in polymers nucleating and crystallizing on fibers.[17,18] The crystalline branches in these spher-

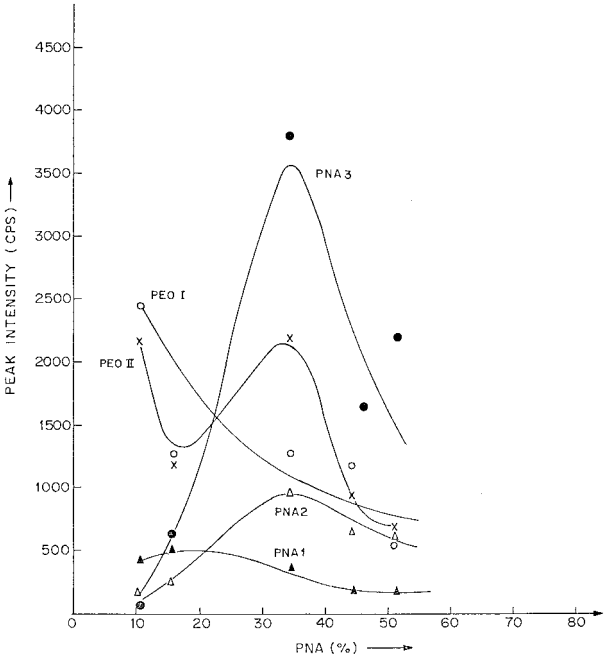

Figure 3 The variation of intensities of the different WAXD peaks in PEO-PNA (SC) films with respect to composition.

ulites are more widely spaced than those in PEO. When the PNA concentration is increased beyond 40%, the morphology changes to a distinctly two-phased type, as shown in Figure 8. It is evident from these micrographs that the samples contain both spherulitic-type as well as tiny, needle-shaped crystals. At even higher concentrations of PNA, that is, beyond 70%, the morphology consists of large, sheaf-like crystals emerging from a nucleating center [Fig. 8(c)]. It is interesting to note that these are highly birefringent (very bright under cross-polarized conditions) and contain thick crystalline arms with a large number of polymer-like crystallites nucleating along their edges, which are distinctly seen at higher magnification [Fig. 8(d)]. These features render them to be quite bright but with nonsharp boundaries at lower magnification; hence, it is difficult to record their micrographs.

In order to confirm the type of interaction between PEO and PNA and to check the possibility of the formation of a complex, the melting points were determined by an optical microscope with hot stage as well as by a differential scanning calorimeter (DSC; the DSC curves are not shown here in order to avoid repetition of data). Figure 9 summarizes the results of melting point determination for different cmopositions of PEO-PNA. It is seen that a single melting point is observed at the extreme compositions ($<35\%$ or $>70\%$ PNA), while for the midrange of compositions (40–70%

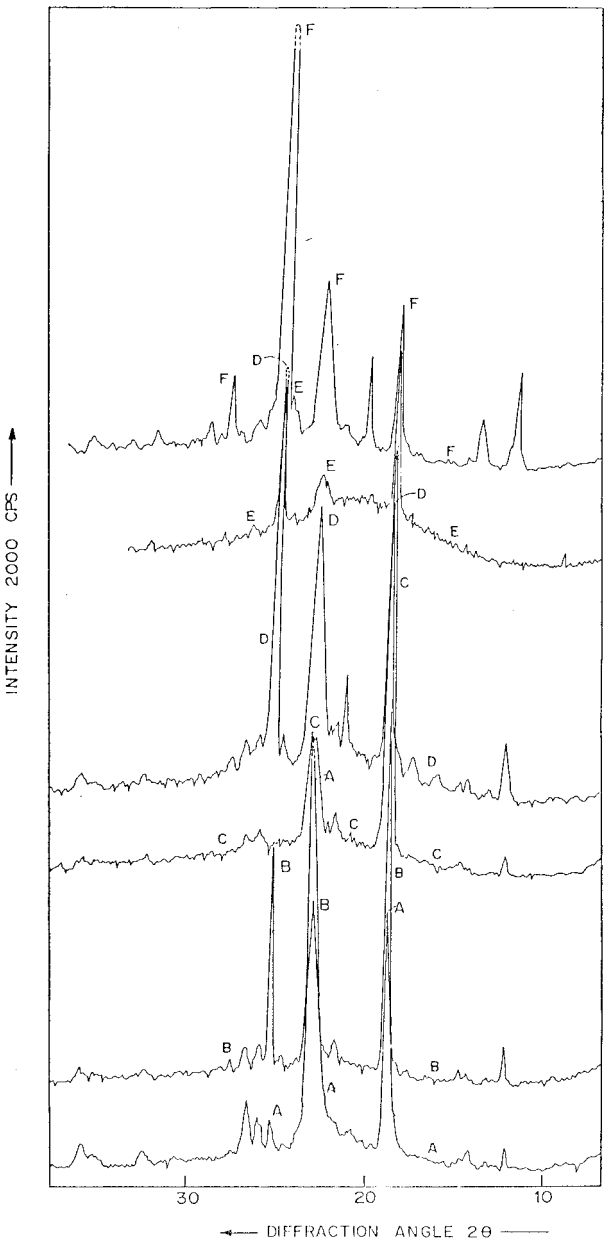

Figure 4 WAXD scans for PEO-PNA (MC) samples with different concentrations of PNA. Curves A–F correspond to PNA concentrations of 10, 15, 25, 35, 45, and 50% by weight, respectively.

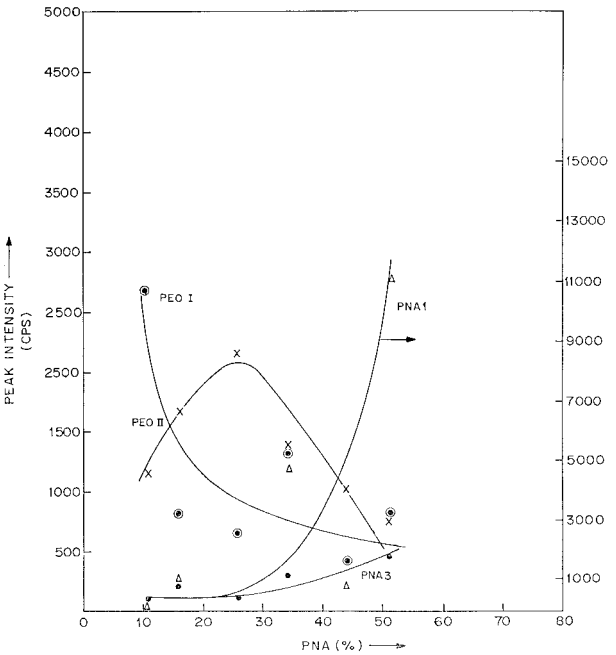

Figure 5 The variation of intensities of the different WAXD peaks in PEO-PNA (MC) films with respect to composition.

PNA), there are two melting points noted: the lower melting point is close to that of PEO while the upper one is likely to be due to the PNA crystals. However, there is significant lowering of the melting points for both components. This can be attributed to dilution effect, which of course presumes large interaction and good miscibility of components. A single melting point at the extreme compositions strongly suggests this possibility. The two melting points at the intermediate compositions can be due to the formation of two types of crystals/two-phase morphology, which in fact has been observed by us [cf. Fig. 8(d)]. It may be mentioned here that the melting behavior has been reported for a number of PEO complexes with inorganic salts as well as urea. In those cases, the new melting peaks in the DSC were observed at certain compositions and these showed entirely new WAXD patterns, suggesting new crystal structure and complex formation. However, in the results presented here, there is no evidence for the new crystal structure but only modification of crystal growth habit.

The infrared (IR) absorption spectra were recorded for the PEO-PNA composite films as well as for the individual components. The comparison of the IR data (obtained from the Fourier transform IR printout) for the PEO-PNA with pure PEO and PNA is made in Table III (the spectra are not shown here so as to avoid repetition). The underlined absorption bands clearly show changes in frequency and intensity; there are shifts of the order of 20–30 cm^{-1} in the N—H stretching (3,360 cm^{-1}), C—N deformation (1,320 cm^{-1}), C—O—C deformation (1,080–1,110 cm^{-1}), and CH_2—O symm (2,830 cm^{-1}) modes. There is also strong absorption at 3,380 cm^{-1}. From these, it can be concluded that the PEO and PNA interact through hydrogen bonding, which takes place at the NH_2 of PNA and the C—O—C moieties of PEO. It may be noted that no entirely new peaks are observed in the IR spectra.

Now PEO and PNA both crystallize in a monoclinic type of structure,[19–21] PEO having lattice parameters of a_p = 8.02 Å, b_p = 13.4 Å, c_p = 19.2 Å, and β_p = 126° and PNA having a_{na} = 12.33 Å, b_{na} = 6.07 Å, c_{na} = 8.59 Å, and β_{na} = 91.45°, respectively. The PNA by itself is a centrosymmetric molecule and crystallizes in antiparallel con-

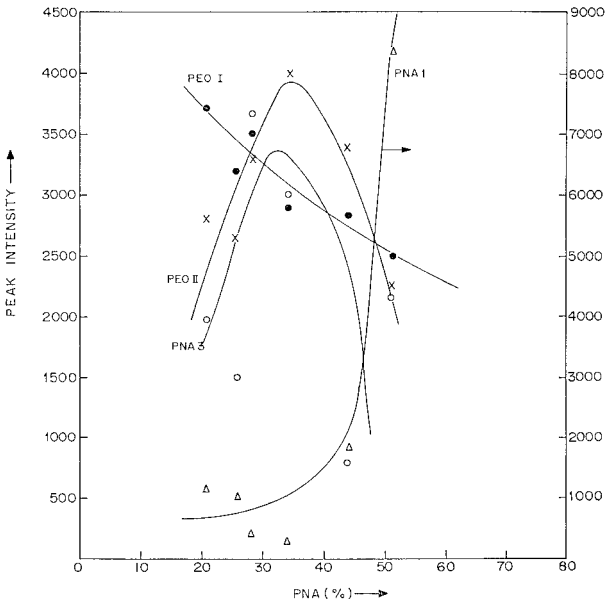

Figure 6 The variation of intensities of the different WAXD peaks in PEO-PNA (PC) samples with respect to composition.

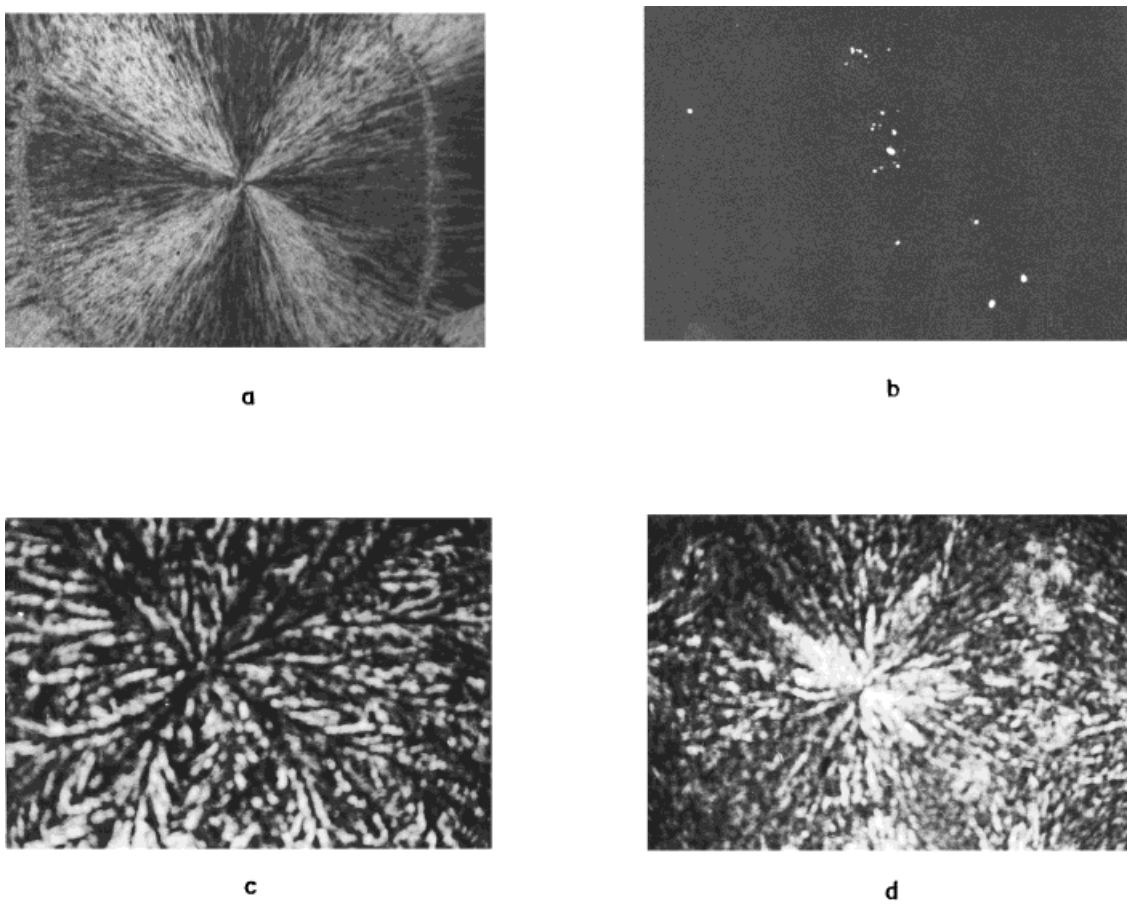

Figure 7 Optical polarizing micrograph for (a) pure PEO, (b) pure PNA, and PEO-PNA (SC) films of (c) 10% and (d) 30% PNA, respectively.

figuration[3,20,21] and hence does not exhibit many NLO second-order effects and has weak birefrengence. According to the lattice mismatch theory, the substrate influences the growth of the overlayer deposited on it if there is a good match between their lattice parameters. In other words, the lattice mismatch (δl) is within certain small limits).[22,23]

$$\delta l = [|n l_s - m l_g|/|l_s| \times 100] < 15\% \quad (1)$$

where δl is lattice mismatch, l_s and l_g are lattice parameters for the substrate and growing medium, respectively, and n and m are integers. In this case, if one considers the mismatch between a_p of PEO and c_{na} of PNA ($|a_p - c_{na}|/|a_p|$), it is 7.1%. Further, the mismatch between b_p of PEO and a_{na} of PNA ($|b_p - a_{na}|/|b_p|$) is 7.9%. These are well within the limits required from eq. (1). It may be mentioned here that PEO also has a strong tendency for complex formation with compounds containing (NH_2) groups, for example, urea, through hydrogen bonding between the oxygen atom of PEO and the NH_2 group of urea.[24,25] Similar interactions can be expected for PEO with PNA as well. However, as mentioned above, although a hydrogen bonding–type interaction exists in these, there is no new crystalline structure observed in the WAXD. Thus, the complex formed through hydrogen bonding does not appear to be crystalline in nature in this case. Hence, it would not directly contibute to the melting peaks or the WAXD data. Nonetheless, the crystallization behavior and resulting morphology are greatly affected by the presence of PEO in the solution or in the melt. One may consider that one component

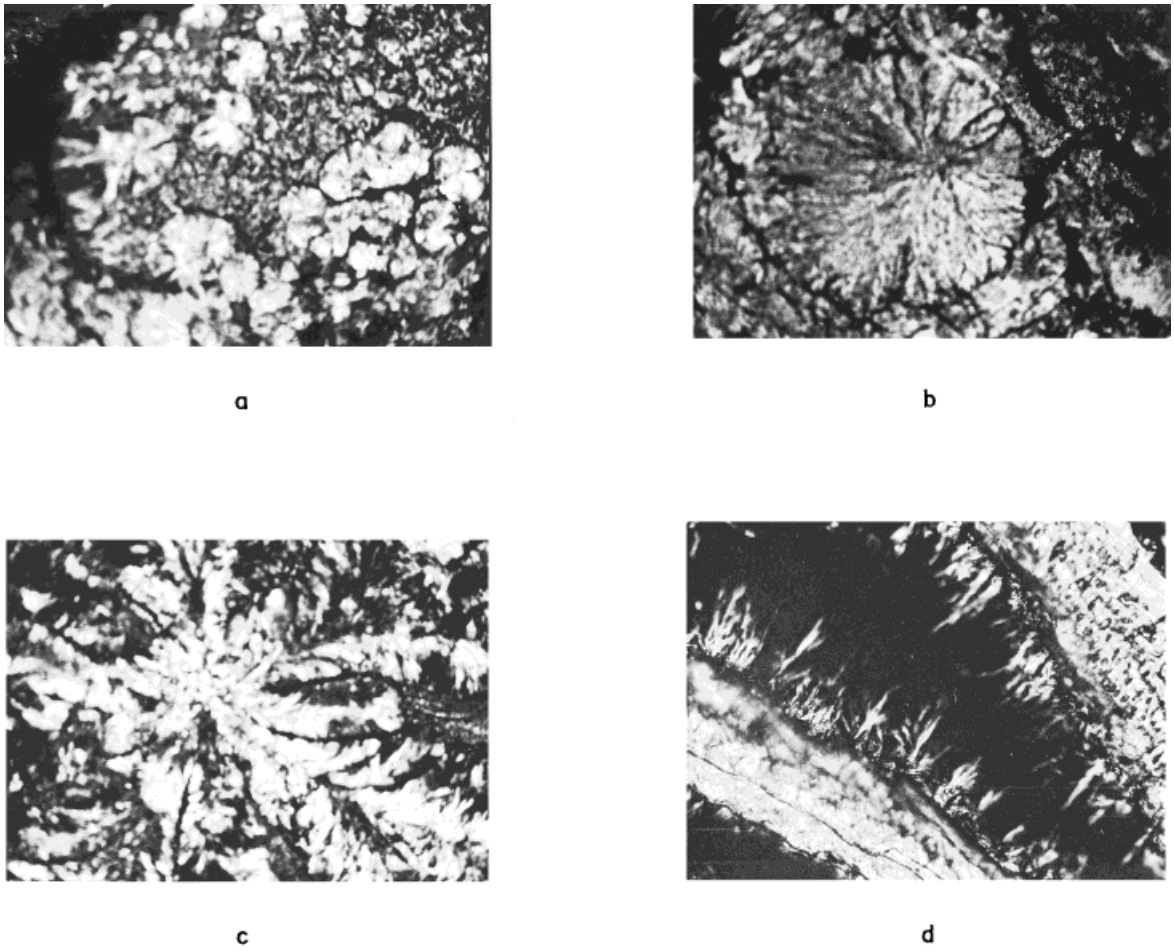

Figure 8 Optical polarizing micrographs for PEO-PNA (SC) films containing (a) 40%, (b) 60%, and (c) 70%, respectively. Panel d is the same as panel c, but at higher magnification.

would be crystallizing out first and acting as a substrate for the other. However, the crystallization and growth of the first component itself are affected due to the interactive molecules present in the solution. Since there is a good lattice match between the $\{\overline{ab}\}$ planes of PEO and the $\{\overline{ac}\}$ planes of PNA, one expects large changes in the growth pattern along the same directions, leading to changes in intensities of the peaks corresponding to reflections such as 120 of PEO and 101 of PNA. This indeed has been observed by us in these studies for the (SC) and (PC) samples, wherein 120 reflection (peak II) of PEO and 101 reflection of PNA (peak 3) exhibited large changes in their intensities. Thus, the crystallites in PEO-PNA composite films are constrained to grow along a certain direction due to mutual interaction between them.

CONCLUSIONS

The crystallization behavior of PEO dispersed with PNA crystals was investigated. The X-ray diffraction patterns show large variations in the intensities of certain peaks with respect to composition and the method of crystallization used. In solution cast films, the 101 reflection from PNA crystallites becomes very intense while the 012 reflection is suppressed, especially at high concen-

Table III IR Absorption of 3 : 1 PEO-PNA Complex as Compared with Pure Components

PEO	PNA	PEO-PNA	Remarks
	3,500 (ms)		
	3,360 (s)	3,380 (vs, br)	N—H stretch and hydrogen bonding
	3,200 (vvw)	3,200 (sh)	
	2,900 (s)		
2,830 (s, br)	2,860 (sh)	2,860 (s)	CH_2—O deformation
1,950 (m, br)			
1,645 (sh)			
1,615 (m)	1,625 (s)	1,620 (sh)	
1,585 (m)	1,590 (s)	1,590 (vvs)	—R cissor NO_2
1,500 (sh)	1,490 (sh)		
	1,475 (s)	1,475 (s)	NO_2 asym. stretch
1,435 (s)	1,440 (sh)	1,440 (sh)	
	1,390 (sh)		C—NH_2 stretch
	1,360 (sh)		
1,340 (s)		1,340 (sh)	CH_2 wagging
	1,320 (sh)	1,300 (vvs)	
1,280 (s)	1,280 (vvs)		
1,235 (sh)		1,240 (sh)	
	1,180 (ms)	1,175 (sh)	C—O—C deformation
1,125 (s)	1,130 (sh)	1,130 (sh)	C—O—C deformation
1,110 (vs)	1,110 (s)	1,100 (s)	
1,080 (vs)		1,050 (sh)	C—O—C deformation
1,030 (ms)		1,025 (sh)	
	995 (vvw)	990 (ms)	δCH out-of-plane deformation aromatic ring
	965 (vvw)		
950 (s)	955 (vvw)	935 (ms)	
835 (s)	840 (ms)	840 (ms)	
	820 (sh)	810 (sh)	δCH out-of-plane deformation aromatic ring
		780 (sh)	
	752 (ms)	750 (ms)	

s, strong; m, medium; v, very; br, broad; sh, shoulder.

tration of PEO. The intensities of the two major peaks from the polymer crystallites also gets affected. The MC show different behavior wherein the 012 reflection of PNA is most intense while the 101 is of medium level. The PC exhibit a mixed trend as compared with SC or MC. The morphology of PEO-PNA films changes considerably with composition. At a low concentration of PNA, the morphology consists of large spherulites similar to those of PEO but differing in their internal structure. At intermediate concentrations, the films have two-phase morphology with one spherulitic and the other prismatic. On the other hand, at a high concentration of PNA (>60%), the morphology again consists of a spherulite-like arrangement of large, sheaf-type crystals. However, each strand contains long, thick crystals with polymer-like dendrites emerging from its sides.

These various results can be explained on the basis of molecular interaction between PEO and NH_2 groups of PNA, as well as the close lattice match between the crystallite of the two components. The former tends to align the molecules during the early stages of crystallization, while the latter leads to preferential growth of the crystals along certain planes.

It is interesting to mention here that PNA by itself is centrosymmetric and crystallizes in the configuration with the molecules arranged alternatively in antiparallel manner.[3,20,21] This leads to weak birefringence and low NLO properties. On the other hand, when it is crystallized in the presence of PEO, highly birefringent crystals are obtained.

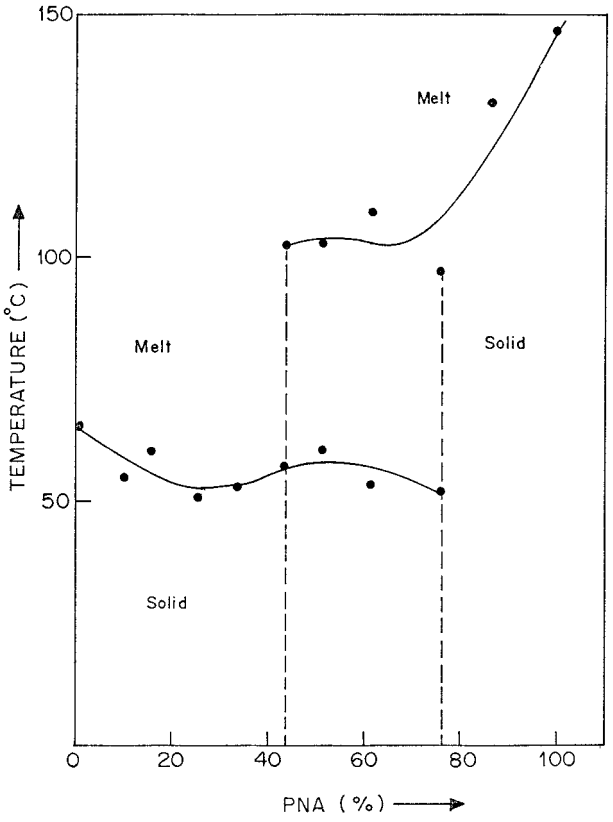

Figure 9 Melting behavior of PEO-PNA composites for different compositions.

This can be due to the preferential growth of certain planes and/or the rearrangement of PNA molecules in all parallel configurations. This suggests an interesting possibility of enhancing the NLO properties of certain crystals using suitably chosen polymers as the growth media.

The authors acknowledge the financial support given by the Department of Science and Technology, New Delhi, for this project.

REFERENCES

1. R. W. Munn and C. N. Ironside, *Principles and Applications of Nonlinear Optical Materials,* Blackie Academic, London, 1993.
2. M. J. Bowden and S. Turner, *Electronic and Photonic Applications of Polymers,* ACS, Washington, DC, 1988.
3. R. A. Hann and D. Bloor, *Organic Materials for Non-linear optics,* Royal Society of Chemistry London, 1989.
4. G. R. Mohlmann, *Synth. Metals,* **37,** 207 (1990).
5. A. Jones, J. R. Hills, and P. Pantelius, in *High Value Polymers,* A. H. Fawcett, Ed., RSC Publications, London, 1991.
6. R. Wan, G. O. Carlisle, K. Koch, and D. R. Martinez, *J. Mater. Sci. Mater. Electron,* **228** (1995).
7. N. Azoz, P. D. Calvert, M. Kadin, A. J. Mccaffery, and K. R. Seddon, *Nature,* **344,** 49 (1990).
8. F. Li, K. Kim, J. J. Kulig, E. P. Savitski, and K. D. Singer, *J. Mater. Chem.,* **5,** 253 (1995).
9. T. Watanabe, K. Yoshinaga, and D. Fichou, *J. Chem. Soc. Chem Comm.,* **250,** (1988).
10. T. Shimizu and N. Sonoda, Jpn. Pat. 02173729 (1990).
11. H. Nakanishi, M. Kagami, N. Hamazolu, T. Watanabe, H. Sato, and S. Miyata, *Proc. SPIE Int. Soc. Opt. Eng.,* 84 (1990).
12. G. T. Bay, C. V. Francis, J. E. Trend, and D. A. Ender, *J. Opt. Soc. Am. B (Opt. Eng),* **8,** 887 (1991).
13. S. Radhakrishnan and J. M. Schultz, *J. Cryst. Growth,* **116,** 378 (1992).
14. J. C. Wittman and P. Smith, *Nature,* **352,** 414 (1991).
15. S. Radhakrishnan and D. R. Saini, *J. Cryst. Growth,* **129,** 191 (1993).
16. S. Radhakrishnan and R. Joseph, *Ferroelectrics,* **142,** 189 (1993).
17. B. Wunderlich, *Macromolecular Physics,* Vol. 182, Academic Press, New York, 1976.
18. J. L. Thompson and A. A. Van Rooyen, *J. Mater. Sci.,* **27,** 889 (1992).
19. H. Tadokoro, F. Yoshihara, Y. Chatani, S. Tahara, and S. Murahast, *Makmol. Chem.,* **73,** 104 (1964).
20. W. G. Wykoff, *Crystal Structure,* Vol. 6, Wiley, New York, 1969.
21. J. Schmierer, G. Jeffrey, and G. J. McCarthy, *Powder Diffr.,* **3,** 98 (1988).
22. A. G. Walton, in *Nucleation,* ZettelMoyer, Ed., Marcel Dekker, New York, 1969.
23. K. A. Mauritz, E. Baer, and A. J. Hopfinger, *J. Poly. Sci. Macromol. Rev.,* **13,** 1 (1978).
24. F. E. Bailey and H. G. France, *J. Polym. Sci.,* **49,** 397 (1961).
25. H. Tadokoro, T. Yoshihara, Y. Chatani, and S. Murahashi, *J. Polym. Sci. Pt. B.,* **2,** 363 (1964).